

data indicate that the multipath effects from the SO truss segment should not be of concern to the ISS GPS antenna performance.

References

- ¹Cohen, C. E., "Attitude Determination Using GPS," Ph.D. Dissertation, Dept. of Aeronautics and Astronautics, Stanford Univ., Stanford, CA, Dec. 1992.
- ²Marhefka, R. J., and Silvestro, J. W., "Near Zone—Basic Scattering Code User's Manual with Space Station Applications," NASA CR-181944, Dec. 1989.
- ³Gomez, S. F., Panneton, R. J., Saunders, P. E., Hwu, S. U., and Lu, B. P., "GPS Multipath Modeling and Verification Using Geometrical Theory of Diffraction," *Proceedings of ION GPS-95*, Inst. of Navigation, Alexandria, VA, 1995, pp. 195–204.
- ⁴Tranquilla, J. M., Carr, J. P., and Al-Rizzo, H. M., "Analysis of a Choke-Ring Groundplane for Multipath Control in Global Positioning System (GPS) Applications," *IEEE Transactions on Antennas and Propagation*, Vol. 42, No. 7, 1994, pp. 905–911.

R. B. Malla
Associate Editor

Mercury Mission Design Using Solar Electric Propulsion Spacecraft

Craig A. Kluever* and Mudar Abu-Saymeh†
University of Missouri—Columbia/Kansas City,
Kansas City, Missouri 64110-2499

Introduction

THE advantages of using low-thrust electric propulsion (EP) for interplanetary missions that require a large energy change have been documented.¹ Several studies have demonstrated the payload enhancements associated with utilizing EP for transfers to the outer planets. For example, previous mission studies include a manned Mars mission² and scientific missions to Jupiter, Uranus, Neptune, and Pluto.^{3,4} In addition, the first New Millennium mission will use solar electric propulsion (SEP) as the primary propulsion mode for transferring a spacecraft to an asteroid.⁵ However, few mission studies have investigated the use of EP for transfers to the inner planets, and, to our knowledge, no research involving a low-thrust rendezvous with Mercury using SEP has ever been published.

In this Note, the feasibility of using SEP for a Mercury mission is investigated by computing the optimal orbit transfers that maximize the spacecraft payload mass at Mercury rendezvous. The proposed Mercury rendezvous is a Discovery-class mission that utilizes Delta and Med-lite launch vehicles for injection into heliocentric space. The EP system consists of 30-cm ion thrusters that are similar to the proposed thrusters for the first New Millennium mission.⁵ For this analysis, the orbit transfer is governed by two-body dynamics, and a gravity assist from Venus is included to reduce further the orbital energy enroute to the Mercury rendezvous. Numerical results are presented for maximum payload trajectories.

Spacecraft System Analysis

The payload mass can be computed as the net mass m_{net} , which is defined as

$$m_{\text{net}} = m_0 - m_{\text{prop}} - m_{\text{tank}} - m_{\text{pp}} \quad (1)$$

Presented as Paper 97-173 at the AAS/AIAA Space Flight Mechanics Meeting, Huntsville, AL, Feb. 10–12, 1997; received Nov. 13, 1997; revision received Feb. 24, 1998; accepted for publication Feb. 24, 1998. Copyright © 1998 by the American Institute of Aeronautics and Astronautics, Inc. All rights reserved.

*Assistant Professor, Mechanical and Aerospace Engineering Department, Member AIAA.

†Graduate Research Assistant, Mechanical and Aerospace Engineering Department.

where m_0 is the injected mass into heliocentric space, m_{prop} is the total SEP propellant mass, m_{tank} is the tank mass, and m_{pp} is the SEP power- and propulsion-system mass. The spacecraft's net mass represents the usable mass for payload plus the basic spacecraft structural mass, which includes "housekeeping" functions such as communication and thermal protection. The basic structural mass can be computed² as a percentage (5–10%) of the initial mass m_0 . Injected mass m_0 is computed via launch performance curves for the Delta and Med-lite vehicles with launch energy C_3 as the independent variable. The tank mass m_{tank} is assumed to be 15% of the propellant mass m_{prop} , and the power- and propulsion-system mass m_{pp} is a function of the input power at 1 AU (P_0) and specific mass (α). The parameter α is fixed at 35 kg/kW for this analysis, which represents the near-term SEP technology level.⁶

It is assumed that xenon is utilized as the propellant for the EP system and that thruster efficiency η is 66% and specific impulse I_{sp} is 3360 s, which corresponds to the SEP system for the first New Millennium mission.⁵ Furthermore, it is assumed that I_{sp} is constant over the entire mission, which implies a fixed engine operating point with no throttling. For our preliminary analysis, the input power P for the SEP spacecraft is assumed to behave in an inverse-square relation with radial distance from the sun. Because the orbit transfer is to an inner planet, P increases as radial distance decreases. Furthermore, we assume that power reaches a maximum value of $2P_0$ and that this maximum power level can be maintained by controlling the attitude of the solar arrays when the radial distance is less than 0.7071 AU.

Trajectory Optimization

The objective of the Mercury mission design is to maximize the net mass of the spacecraft at Mercury rendezvous conditions. We assume a fixed heliocentric trajectory sequence that begins with a powered SEP arc near the Earth's sphere of influence (SOI) after chemical injection into heliocentric space followed by a coasting phase that includes a Venus gravity assist and finally a second powered SEP arc to Mercury rendezvous. The insertion into a parking orbit about Mercury is not addressed in this study. The trajectory design variables include the launch date, the hyperbolic velocity vector at the SOI, the durations of the two powered arcs, the thrust direction for the powered arcs, the changes in true longitude for the coast arcs, the planetary flyby conditions, and the rendezvous date. The trajectory is governed by the equations of motion for a thrusting spacecraft in an inverse-square gravitational field. The powered arcs are numerically computed by integrating the equations of motion using a fixed-step, fourth-order Runge–Kutta routine with 100 integration steps for the first powered arc and 500 steps for the second arc. The coast arcs are computed analytically using two-body mechanics. Planetary gravity assists are modeled as instantaneous changes in velocity ΔV without change in spacecraft position. The gravity assist is defined by two free parameters: the periaxis radius and orbit plane orientation for the flyby. Details of the numerical simulation of the trajectory are presented in Ref. 7.

Numerical solutions of the trajectory optimization problem are obtained by utilizing sequential quadratic programming (SQP), a constrained parameter optimization method.⁸ The SQP code used here is taken from Ref. 9 and computes the gradients with forward finite differences. The thrust steering history is defined by three direction cosines, which are parameterized in the optimization problem by linear interpolation through a set of control nodes. Nine SQP equality constraints are imposed: Six constraints maintain the match between the orbital elements of the spacecraft and Mercury at the final end time, and three constraints maintain the match between the position of the spacecraft and Venus at the gravity assist. The planetary elements are computed by a solar system ephemeris.

Results

Maximum Payload Trajectories

Several trajectories maximizing m_{net} are obtained for a range of input power levels P_0 , and the results are shown in Fig. 1. Although the launch date is a free design variable, we chose a nominal launch date in the mid-2002 time frame. Optimal transfers are obtained for

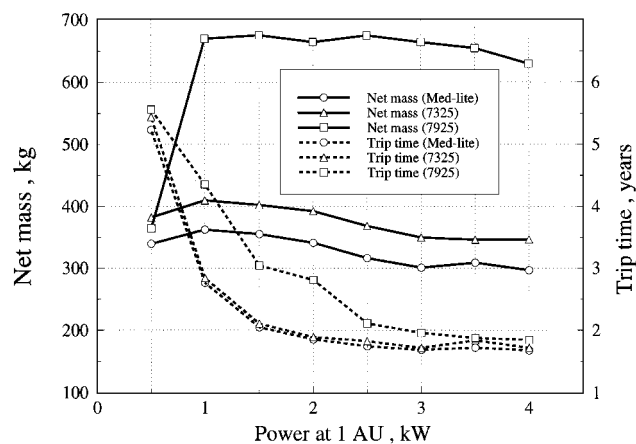


Fig. 1 Maximum net mass and trip time vs SEP power at 1 AU.

three launch vehicles: Delta 7925, Delta 7325, and Med-lite. The Delta 7325 can deliver roughly 58% of the injection mass of a Delta 7925 for the same C_3 , whereas the Med-lite performance is about 53% of that of the Delta 7925 for the same C_3 . Each data point in Fig. 1 represents a trajectory solution that maximizes m_{net} for a fixed P_0 . Figure 1 demonstrates how optimal m_{net} dramatically increases for the Delta 7925 as P_0 is increased from 0.5 to 1.0 kW and then remains between 675 and 630 kg in the 1–4-kW range. The optimal payload characteristics for the other two launch vehicles do not exhibit a dramatic variability, for P_0 and m_{net} range from 362 to 297 kg for the Med-lite and from 410 to 346 kg for the Delta 7325. Note that the optimal m_{net} is within 50 kg for the missions using the Med-lite and Delta 7325 vehicles; this is because the launch energy C_3 is comparable for these two mission design sets, which results in a 50-kg difference in injected mass m_0 .

Note that the solutions presented in Fig. 1 are not minimum-fuel solutions, nor is it desirable to obtain minimum-fuel solutions because m_0 is not fixed. If the EP propellant mass were minimized, a large portion of the energy change would be performed by the upper stage of the launch vehicle (that is, C_3 would be large), so that the remaining orbital transfer using the SEP stage would be minimized. Therefore, because m_{net} is maximized, C_3 is reduced (which increases m_0), so that the majority of the orbit transfer is performed by the more efficient SEP stage. The optimal payload solutions demonstrate that, as P_0 is increased, m_0 increases (C_3 decreases) and m_{prop} increases (which indicates that the SEP stage is performing a greater percentage of the orbit transfer).

Figure 1 also presents the corresponding total trip time for the mission as P_0 changes. Total mission time exhibits a sharp decrease with increasing P_0 for all three launch vehicles. Figure 1 shows that trip time is in excess of five years for $P_0 = 0.5$ kW for all three vehicles. This is due to the long-duration powered inward spiral to Mercury's orbit that follows the Venus gravity assist. As the power level is increased, the inward spiral time is decreased, and therefore total trip time is reduced. When P_0 is less than 1 kW, the trip time is greater than three years for the Med-lite and Delta 7325 missions, and the trip time exceeds three years when P_0 is less than 1.5 kW for missions using the Delta 7925. These trip times are probably excessive for the Discovery mission time frame. Figure 1 also shows that trip time levels off and m_{net} slightly decreases as power is increased past 2 kW. Therefore, the best tradeoff between payload performance and trip time occurs at $P_0 = 1.5$ kW for missions using the Med-lite and Delta 7325 and at $P_0 = 2.5$ kW for missions using the Delta 7925.

Thruster Lifetime Constraints

Another mission design consideration is thruster lifetime. The ion thrusters for this study are based on the EP system proposed for the first New Millennium mission and are able to eject a maximum m_{prop} of about 83 kg per thruster before grid erosion renders the thrusters unusable. All optimal mission designs from the preceding section (with the exception of the Med-lite mission with $P_0 = 0.5$ kW) exceeded a two-thruster propellant mass limit of 166 kg, and most

Table 1 Maximum net mass transfers with propellant constraints

Vehicle	P_0 , kW	Launch date	C_3 , km ² /s ²	m_0 , kg	$m(t_f)$, kg	m_{net} , kg	Trip time, yr
Med-lite ^a	1.5	Sept. 1, 2002	8.1	579.6	413.6	336.2	2.02
Delta 7325 ^a	1.5	Sept. 12, 2002	11.9	595.7	429.7	352.3	2.02
Delta 7925 ^a	2.5	Oct. 22, 2002	44.4	521.6	355.6	243.2	1.62
Delta 7925 ^b	2.5	Aug. 24, 2002	5.9	1138.6	806.6	669.3	2.10

^aPropellant mass $m_{\text{prop}} \leq 166$ kg. ^bPropellant mass $m_{\text{prop}} \leq 332$ kg.

of the Delta 7925 missions exceeded a four-thruster limit of 332 kg. Therefore, an additional constraint requiring that $m_{\text{prop}} \leq 166$ kg (and $m_{\text{prop}} \leq 332$ kg for the Delta 7925) was imposed on the maximum net mass problem. The maximum payload trajectories with these propellant constraints are presented in Table 1. We present only solutions for the missions that had previously demonstrated a good tradeoff between payload performance and trip time. During the optimization process, the initial SEP-powered arc was eliminated, and C_3 was subsequently increased so that the Venus flyby was achieved. However, the Venus flyby remains significant even for the third case in Table 1; the Delta 7925 with the 166-kg propellant constraint delivers a reduced payload of only 107 kg without the Venus flyby. The thruster constraint reduces the payload mass by 19 kg for the Med-lite, 50 kg for the Delta 7325, 432 kg for the Delta 7925 with a two-thruster limit, and 6 kg for the Delta 7925 with a four-thruster limit.

The optimal SEP transfers presented here demonstrate significant improvements in payload mass and trip time when compared with Mercury missions that utilize conventional chemical propulsion. An optimal ballistic trajectory for the mid-2002 time frame was computed using the MIDAS program, and the final spacecraft mass at Mercury rendezvous is 210 kg for the Delta 7925 and 124 kg for the Delta 7325. This optimal ballistic trajectory required a three-year trip time with two Venus and two Mercury gravity assists. The respective optimal SEP transfers (with propellant constraints) triple the mass performance of the optimal ballistic transfers and reduce the trip time by about a year.

Conclusions

Several maximum-payload Mercury rendezvous trajectories using SEP have been obtained. The tradeoffs between payload mass, trip time, and input power were identified. In addition, the effects of thruster lifetime constraints on the mission performance were investigated. These preliminary results show that an SEP spacecraft with two ion thrusters is capable of delivering a significant payload mass of about 336 kg to Mercury rendezvous conditions using a Med-lite launch vehicle and 352 kg using a Delta 7325. The input power is 1.5 kW, and trip time is two years for both cases. A mission using a Delta 7925 can deliver a significant payload mass only with a spacecraft with four ion thrusters; the resulting payload mass for this case is 669 kg, and the trip time is about two years. The optimal SEP transfers exhibit a 200% increase in mass performance and a one-year trip time reduction when compared with an optimal all-chemical ballistic transfer for the same launch vehicles. Our preliminary results suggest that a Mercury mission utilizing an SEP spacecraft and a small launch vehicle is feasible and therefore is a potential candidate for a Discovery-class mission.

Acknowledgment

The authors would like to thank Paul A. Penzo at the Jet Propulsion Laboratory, California Institute of Technology, for his many helpful discussions during the course of this work.

References

- ¹Fearn, D. G., "The Impact of Ion Propulsion on High Energy Interplanetary Missions," 45th Congress of the International Astronautical Federation, Paper IAF-94-U.4.487, Jerusalem, Israel, Oct. 1994.
- ²Hack, K. J., George, J. A., and Dudzinski, L. A., "Nuclear Electric Propulsion Mission Performance for Fast Piloted Mars Missions," AIAA Paper 91-3488, Sept. 1991.

³Kelley, J. H., and Yen, C. L., "Planetary Mission Opportunities with Nuclear Electric Propulsion," AIAA Paper 92-1560, March 1992.

⁴Meserole, J. S., and Richards, W. R., "Direct-Trajectory Options Using Solar Electric Propulsion for the Pluto Fast Flyby," AIAA Paper 94-3253, June 1994.

⁵Rayman, M. D., and Lehman, D. H., "NASA's First New Millennium Deep-Space Technology Validation Flight," Second International Academy of Astronautics International Conf. on Low-Cost Planetary Missions, Paper IAA-L-0502, Laurel, MD, April 1996.

⁶Oleson, S. R., "Influence of Power System Technology on Electric Propulsion Missions," AIAA Paper 94-4138, Aug. 1994.

⁷Kluever, C. A., "Optimal Interplanetary Trajectories by Direct Method Techniques," *Journal of the Astronautical Sciences*, Vol. 45, No. 3, 1997, pp. 247-262.

⁸Pierson, B. L., "Sequential Quadratic Programming and Its Use in Optimal Control Model Comparisons," *Optimal Control Theory and Economic Analysis 3*, North-Holland, Amsterdam, 1988, pp. 175-193.

⁹Pouliot, M. R., "CONOPT2: A Rapidly Convergent Constrained Trajectory Optimization Program for TRAJEX," Convair Div., General Dynamics, GDC-SP-82-008, San Diego, CA, Jan. 1982.

J. A. Martin
Associate Editor

Development of a Renewable Atomic Oxygen Sensor for Low Earth Orbit

S. B. Gabriel,* J. J. Osborne,† G. T. Roberts,*
and A. R. Chambers‡

University of Southampton, Southampton,
Hampshire SO17 1BJ, England, United Kingdom

Introduction

THIS Note describes the design, development, and preliminary testing of a reusable atomic oxygen (AO) sensor for use in low Earth orbit (LEO). The most prevalent species in the Earth's thermosphere between the altitudes of approximately 150-650 km is AO.¹ The high orbital velocity of satellites in this region results in large fluxes of high-energy (~5-eV) atoms impinging on ram surfaces. The colliding oxygen atoms may simply scatter off, or they may form excited species that produce a glow that can interfere with the operation of optical systems.² Last, AO may erode exposed surface materials.³ AO erosion results in mass changes; frequently other characteristics, such as the thermal radiative properties of materials, may also be changed.⁴ Thus, changes of satellite temperature, contamination due to polymer chain fragmentation, and loss of power-generating capability may occur as a consequence of AO erosion.³ Clearly, there is a requirement to develop sensors that can be used to characterize the AO environment that satellites experience.

Atomic Oxygen Measurement

Several techniques for measuring the AO environment have been developed. In general, an ideal sensor would be lightweight, small, accurate, and stable; would require low power; and would give time-resolved measurements of the AO flux. The simplest way of measuring AO exposure is to use a witness sample of a material whose erosion yield is well known. Although this method is lightweight, it suffers from many disadvantages; it can only give an indication of the total AO fluence and requires retrieval. Quartz crystal microbalances (QCMs) can provide a remote measurement of AO

flux,⁵ but their mass and power often make them unsuitable for small satellites, especially for multiple sensor operations.⁶ Both witness samples and QCMs suffer from inaccuracies in material erosion yield values and from the fact that they can only be used for one set of measurements. Mass spectrometers have been used to characterize the ambient atmosphere and also AO/material reaction products.^{7,8} Although they can give time-resolved readings of many species, they tend to be heavy and bulky and require considerable power, which often makes them unfeasible for microsatellite missions.

Thin film resistance sensors (actinometers) can be used to detect AO.⁹ The resistance of a thin conducting film depends on its thickness and other dimensions. If such a film is reactive with AO, surface erosion reduces the conductor thickness, thereby causing a resistance increase. Films of silver have been used in this way; however, the AO fluence that can be measured by such films is restricted by a diffusion-limited regime due to the presence of an insulating oxide layer that forms on the conductor surface.¹⁰ Carbon, which has volatile oxides (and thus does not suffer from the same problem as silver), has also been used.¹¹ Actinometers offer a simple, low-power, lightweight method and have been adapted for microsatellite use.^{6,12} However, these sensors can only be used once and as a result of their low sensitivity can only record the AO fluence. Thus it seems that none of the sensors used to date satisfies the requirements of an ideal sensor.

Semiconducting Sensors

Semiconducting detectors (SCDs) have been used for gas detection since the discovery that the chemisorption of species onto the surface of a semiconductor changes the electrical characteristics of that sample, particularly the conductivity.¹³ If thin films of the semiconductor are used, the induced surface changes dominate the bulk effects, and the detection of the surface conductivity is made easier. Commonly, metal oxide semiconductors have been used because the ionic structure of these materials means they have large band gaps and therefore a low number of intrinsic charge carriers. The majority of charge carriers are therefore extrinsic, and so the conductivity of the semiconductor sample is highly sensitive to any form of doping.

One of the main benefits of semiconductor sensors (apart from their light weight and small size) is the ability to regenerate their pre-exposure properties by heating, allowing the sensors to be reused many times.¹⁴ Because resistance measurements are used as the gauge of chemisorption and hence AO exposure, they, like actinometers, require low power. However, unlike actinometers, SCDs can have high sensitivities; for example, the sensitivity of zinc oxide to AO has been found to be 10^9 - 10^{10} atoms $\text{cm}^{-2} \text{s}^{-1}$ compared with $\sim 10^{15}$ atoms $\text{cm}^{-2} \text{s}^{-1}$ for silver films^{15,16} (based on the data in Ref. 16 and the assumption that the pulsed AO source was run at ~3 Hz). Thus it would seem that a sensor based on semiconducting metal oxides may satisfy most of the criteria of an ideal sensor.

Such sensors have been adapted for pulsed-mode AO sensing in the lower thermosphere on board a sounding rocket¹⁵ but, so far, have not been used continuously in space. The remainder of this Note will describe the development of a microsatellite experiment based on SCDs.

Experimental Development

Laboratory testing in the pulsed laser AO facility at the European Space and Technology Centre shows that the resistances of zinc oxide single crystals increase under the action of AO flux. The increase in resistance is brought about by the localization of electrons from the conduction band by the adsorbed AO. The resistance increase is also shown to be reversible. Figure 1 is a graph of an exposure/regeneration cycle for a single crystal. It can be seen that the rate of resistance change increases when the AO flux was switched on and stops increasing when the AO was switched off and the regeneration commenced. The same figure shows the temperature of the crystal during exposure and the effect of heating the crystal to ~350 K: it is evident that, when the sensor reaches the temperature recorded before AO exposure, the resistance of the

Received Dec. 23, 1997; revision received Feb. 25, 1998; accepted for publication March 13, 1998. Copyright © 1998 by the American Institute of Aeronautics and Astronautics, Inc. All rights reserved.

*Senior Lecturer, Department of Aeronautics and Astronautics.

†Research Assistant, Department of Aeronautics and Astronautics.

‡Lecturer, Department of Engineering Materials.